JOURNAL OF DEGRADED AND MINING LANDS MANAGEMENT
ISSN: 2339-076X (p); 2502-2458 (e), Volume 6, Number 3 (April 2019):1789-1802
DOI:10.15243/jdmlm.2019.063.1789

Research Article

The dynamics of shoreline change analysis based on the integration of remote sensing and geographic information system (GIS) techniques in Pekalongan coastal area, Central Java, Indonesia

Fajar Yulianto*, Suwarsono, Taufik Maulana, Muhammad Rokhis Khomarudin

Remote Sensing Application Center, Indonesian National Institute of Aeronautics and Space (LAPAN), Jl. Kalisari No. 8, Pekayon, Pasar Rebo, Jakarta 13710, Indonesia.

*corresponding author: fajar.lapan.rs@gmail.com, fajar.yulianto@lapan.go.id

Received 13 February 2019, Accepted 12 March 2019

Abstract: Coastal areas are found in the dynamic zone at the interface between the three major natural systems of the Earth's surface. The phenomenon of shoreline change is one of the most frequent problems encountered in the coastal environment and is caused by natural processes that result in dynamic changes in the coastal area. Coastal area change can affect the vulnerability of the coastal environment and its properties, such as shoreline stabilization, flood control, sediment retention, natural protection and others. The method of integrating remote sensing data with geographic information system (GIS) techniques has been widely used to monitor and analyze the dynamics of shoreline change in coastal areas. The purpose of this study is to map and analyze the dynamics of shoreline change from 1978 to 2017 in the study area. An approach combining spectral value index and visual interpretation of Landsat images was used and proposed to indicate the separation of land and water bodies, for shoreline extraction. The normalized difference water index (NDWI) can be used as a spectral value index approach for differentiating land and water bodies. Furthermore, the analysis of shoreline changes was performed using the digital shoreline analysis system (DSAS). Based on calculations made using DSAS, it can be seen that the pattern of coastline change tends to be dominated by offshore erosion. The results of this study may also be important as input data for coastal hazard assessment as part of the effort to overcome the problem of flood tides.

Keywords*: dynamics of shoreline change, GIS, remote sensing, tidal flood*

To cite this article: Yulianto, F., Suwarsono, Maulana, T. and Khomarudin, M.R. 2019. The dynamics of shoreline change analysis based on the integration of remote sensing and geographic information system (GIS) techniques in Pekalongan coastal area, Central Java, Indonesia. J. Degrade. Min. Land Manage. 6(3): 1789-1802, DOI: 10.15243/jdmlm. 2019.063.1789.

Introduction

The phenomenon of shoreline change is one of the most frequent problems encountered in the coastal environment and is caused by natural processes that result in dynamic changes in coastal area (Thomas et al., 2015; Burningham and French, 2017). Coastal area change can affect the vulnerability of the coastal environment and its properties, such as shoreline stabilization, flood control, sediment retention, natural protection and others (Marfai and King, 2007; Bonetti et al., 2013; Brown et al., 2013). In addition, changes in the coastal environment can also be caused by human construction activities including the development of infrastructure facilities. According to Bird and Ongkosongo (1980) and Marfai and King (2007), the development of seawalls and breakwaters, artificial coastal land reclamation and the removal of coastal materials have direct impacts on changes in the coastal environment.

Remote sensing data archives integrated with GIS techniques can be used to track and historically map the dynamics of coastal shoreline change. Remote sensing data integrated with GIS techniques have been widely used to monitor and analyze the dynamics of shoreline changes in

coastal areas, including Landsat MSS, TM and SPOT imagery (Marfai and King, 2007; Li and Damen, 2010; Erener and Yakar, 2012), ASTER imagery (Addo et al., 2011; Allen, 2012), Ikonos imagery (Kaichang et al., 2004), Quickbird imagery (Xiaodong et al., 2006) and others.

Pekalongan is located in the coastal area of Central Java, Indonesia. Study of the characteristics of dynamic shoreline change is important for the coastal areas of Pekalongan. The purpose of this study is to map and analyze the dynamics of shoreline change from 1978 to 2017 based on the integration of remote sensing and GIS techniques in the study area. This study was conducted as part of the effort to overcome the problem of flood tides, focusing on the exploration and analysis of the dynamic characteristics of coastal shoreline change as one of the causes of tidal flooding in Pekalongan. In addition, the results of this study may also be important as input data for coastal hazard assessment.

Study area

The study area is located in Pekalongan which is in one of the northern coastal areas of Central Java, Indonesia (Figure 1) at coordinates 6º 51' 00" S–6º 54' 00" S and 109º 36' 00" E–109º 43' 00" E. In general, the geological formations in the study area are alluvial deposits derived from rivers and swamps and beaches with a thickness of up to 150 m consisting of gravel, sand, silt and clay (Condon et al., 1996).

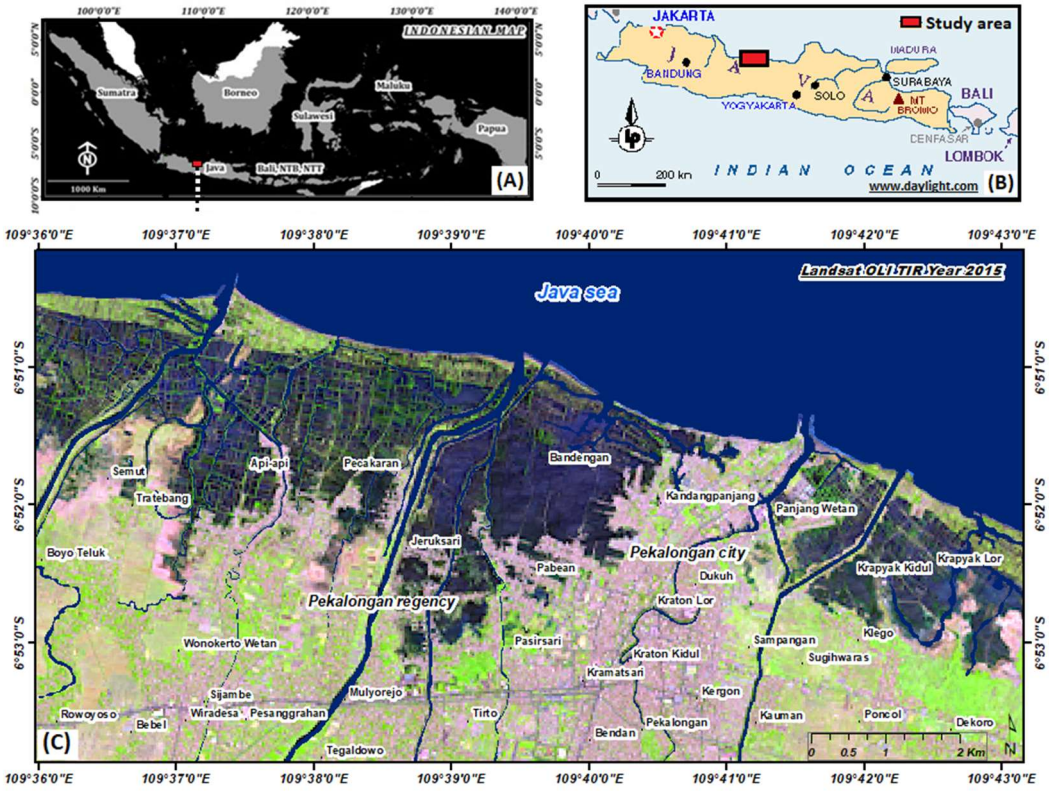

Figure 1. The study area is located in the coastal area of Pekalongan, Central Java, Indonesia: (A) Map of Indonesia; (B) Inset map of the study area; (C) Coastal area of Pekalongan from Landsat OLI/TIR, 2015

Materials and Methods

Data availability

In this study, remotely sensed data were used to perform shoreline mapping and analysis. Landsat data, with a resolution of 30 m at Level 1 Geometric (L1G) with sensor MSS (path/row: 120/65) was used as the input data for 1978 while TM sensor data was used for 1988, 2007 and 2011. The ETM + sensor was used as the input data for 2000 and OIL/TIRS sensors was used as the input data for 2017. Landsat MSS and Landsat 5 TM data were provided by the US Geological Survey (USGS) and Landsat 7 ETM + and Landsat 8 OLI/TIR data were provided by the Remote Sensing Technology and Data Center, LAPAN.

Image and ancillary data pre-processing

Satellite image pre-processing was performed to convert the digital number (DN) values to reflectance values. The standard products Landsat MSS, 5 TM and 7 ETM + provide data in 8-bit unsigned integer format while Landsat 8 OLI/TIRS provides 16-bit unsigned integer data. Processing into standard reflectance is required to address these differences in value formats in satellite images. The first stage of the conversion process converts DN values to radian values using the formula presented in Equation 1. The second stage converts radian values to reflectance values, as in Equation 2. This second stage of the process refers to Chavez (1988), NASA (2011), USGS (2013a, 2013b), and Yulianto et al. (2016).

$$L_\lambda = [\frac{(Lmax_\lambda - Lmin_\lambda)}{(Q_{Calmax} - Q_{Calmin})}] \, x \, (Q_{Cal} - Q_{Calmin}) + Lmin_\lambda \quad (1)$$

where L_λ is spectral radiance at the sensor's aperture; Q_{Cal} is quantized calibrated pixel value; $Lmin_\lambda$is spectral radiance scaled to Q_{Calmin}; $Lmax_\lambda$ is spectral radiance scaled to Q_{Calmax}; Q_{Calmin} is minimum quantized calibrated pixel value and Q_{Calmax} is maximum quantized calibrated pixel value.

$$\rho = [\pi x (L_\lambda - L_\rho) x d^2] / (ESun_\lambda x Cos\theta_s) \quad (2)$$

where ρ is the land-surface reflectance for Landsat images; L_λ is satellite radiance; $L_\rho$is path radiance; d is Earth-to-Sun distance in astronomical units; $ESun_\lambda$ is mean solar exo-atmospheric irradiance and θ_s s is the solar zenith angle.

The dynamics of coastal shoreline mapping and change analysis

Shoreline mapping and change analysis are important in providing input data for coastal hazard assessment (Marfai et al., 2007). Several studies have been conducted with various approaches for shoreline extraction using integration of remote sensing data and GIS techniques, including visual interpretation, spectral value index, multi-source data analysis, automatic change detection, change vector analysis and others (Kalliola, 2004; Shalaby and Tateishi, 2007; Ekercin, 2007; Erkkilä and Marfai et al., 2007; Zhao et al., 2008; Kuleli et al., 2011).

In this study, an approach combining spectral value index and visual interpretation of Landsat images was used and proposed to indicate the separation of land and water bodies, for shoreline extraction. The normalized difference water index (NDWI) can be used as a spectral value index approach for differentiating land and water bodies, as used by Memon et al. (2015). According to Gao (1996), the NDWI is one of the indicators sensitive to the change in water content and can be used to detect objects related to water bodies, as derived from near-infrared (NIR) and short-wave infrared (SWIR) channels of remote sensing data. In this study, the NDWI value can be derived and used for the Landsat 5 TM images for 1988, 2007 and 2011, for Landsat 7 ETM+ for 2000 and for Landsat 8 OLI/TIR images for 2017. NDWI can also be derived from NIR and green channels in remote sensing data (McFeeters, 1996). In this study, the NDWI value can be used for the Landsat MSS images for 1978. In detail, the equation for obtaining NDWI values based on remote sensing channels refers to previous studies conducted by Gao (1996) for Equation 3 and McFeeters (1996) for Equation 4.

$$NDWI = \frac{\rho NIR - \rho SWI}{\rho NIR + \rho SWIR} \quad (3)$$

$$NDWI = \frac{\rho Green - \rho NIR}{\rho Green + \rho NI} \quad (4)$$

where $\boldsymbol{NDWI}$ is the normalized difference water index; $\boldsymbol{\rho NIR}$ is the near-infrared channel remote sensing data; $\boldsymbol{\rho SWIR}$ is the short-wave infrared channel remote sensing data; and $\boldsymbol{\rho Green}$ is the green channel remote sensing data.

Determination of the threshold value for NDWI is required for this study to separate land and water bodies. According to McFeeters (1996), threshold value needs to be applied to the NDWI so as to eliminate those land areas or non-water surfaces which have low reflectance value. We used the isolation approach for the purest water pixels accomplished by using one or more conditional statements that would both threshold the NDWI (if needed) and eliminate pixels using the threshold value. The conditional test expression 'Con' with the threshold set for the value masking operation is run using the raster calculator tool in the Math Toolset of Spatial Analyst ESRI software, as shown in Equation 5 (McFeeters, 2013). The results of NDWI processing can then be used as a reference for visual interpretation using on-screen digitation, to distinguish between land and water bodies. If the NDWI value is equal to or greater than 'value masking operation', then the pixel is unchanged, but if it is not, then a value of -10 is assigned and it is carried forward to the next element of the expression. If the pixel is exactly equal to the 'zone maximum value of NDWI' found within the parcel, then a value of one is assigned to the output grid cell; if it is not, a value of zero is assigned (McFeeters, 2013).

$$\boldsymbol{binNDWIMax} = \boldsymbol{Con}((\boldsymbol{Con}(\boldsymbol{NDWI} \geq \boldsymbol{valuemaskingoperation}, \boldsymbol{NDWI}, -\mathbf{10})) == \textit{"Zonal Maximum value of NDWI"}, \mathbf{1.0}) \quad \text{..... (5)}$$

Furthermore, the analysis of shoreline changes was performed using the Digital Shoreline Analysis System (DSAS) ver. 4.4 software released in July 2017, as used previously by Carrasco et al. (2012), Rio et al. (2013), Hackney et al. (2013), Thébaudeau et al. (2013), Oyedotun (2014). DSAS is a freely available software application that works within the Environmental Systems Research Institute (ESRI) Geographic Information System (ArcGIS) software. This plug-in ArcGIS extension was developed by Thieler et al. (2017) and can be used for calculating shoreline change. DSAS computes rate-of-change statistics for a time series of shoreline vector data and can be used for historical trend analysis.

Results

In this study, coastal shoreline extraction and mapping were performed based on a combination of NDWI value calculations and visual interpretations of Landsat images. The high NDWI values indicate the high sensitivity of the Landsat image channel for identifying water bodies, as a result of which the boundaries between land and water bodies can be distinguished. Figure 2 shows the NDWI values obtained from Landsat images for 1978 to 2017 used as an indication of the separation of land and water bodies and used for shoreline and river extraction. Table 1 shows the NDWI value statistics used for the masking operation for land and water-body extraction from Landsat images for 1978 to 2017. Furthermore, the separation of land and water bodies and their multi-temporal change analysis are presented in Figures 3, 4 and 5. From Table 1 it can be shown that the available Landsat images have variations in statistical value which affect the threshold masking operation values. The use of high-resolution imagery (e.g., Google Earth, SPOT 6/7 image) is required as a reference to ensure the accuracy of the boundaries between land and water.

The threshold masking operation used for Landsat images has different values for each year, as presented in Table 1. This reflects the different statistical parameters in each dataset. For example, Landsat images for1978 have threshold masking operation value of 0.34. This means that, based on Equation 5, if the NDWI value is equal to, or greater than 0.34, then the pixel is unchanged, but if it is not, a value of -10 is assigned to it and it is carried forward to the next element of the expression. If the pixel is exactly equal to the maximum value of NDWI zone found within the parcel, then a value of one is assigned to the output grid cell; if it is not, a value of zero is assigned.

Table 2 shows the change area and average change results based on the multi-temporal analysis of land and water separation for 1978 to 2017. It can be seen that during the period 1978 to 2017 there was an increase in land area of 106.11 ha, with the average change being 2.72 ha/year. Meanwhile, there was a decrease in the land area of 543.94 ha, with the average change being 13.95 ha/year. The changes in shorelines and the delta have not only been caused by natural factors but also by factors such as the construction of docks and jetties around the mouth of the river (as presented in Figures 3, 4 and 5).

In this study, the segments and transects used for DSAS are presented in Figure 6 and the analysis of the rate-change statistics provided by DSAS used in this study are presented in Table 3. The parameter settings consisting of transect spacing and length in this study is 300 m, with cast direction being auto-detected and a default uncertainty level of 6 m. The DSAS analysis has produced 49 transect IDs, 44 of which are offshore and five are onshore. As shown in Table 3, six parameters are used in the DSAS analysis: end point rate (*EPR*); least median of squares rate (*LMS*); linear regression rate (*LRR*); R-squared of linear regression (*LR2*); standard error of linear regression (*LSE*) and confidence interval of linear regression (for 90%) (*LCI90*).

The DSAS results for the examples transect_ID = 11 (offshore position or erosion) and transect_ID = 25 (onshore position or sedimentation) are presented in Figure 7. In the examples illustrated in Figure 7 and Table 3, it can be interpreted that transect_ID = 11 has *EPR* of -2.81 m/year during the period 1978 to 2017 and *LMS* rate rounded to -2.76 m/year. The linear regression equation for transect_ID = 11 (y = -2.8835x + 5661.7) was determined by plotting the shoreline positions with respect to time (in years) and the slope of the equation describing the line; from this, the *LRR* is -2.88 m/year and the *LCI90* is 0.86. The band of confidence around the reported rate of change is -2.88 ± 0.86. In other words, there is 90% confidence that the true rate of change is between -3.74 m/year and - 2.02 m/year, with *LR2* of 0.95 and *LSE* of 8.15 m.

Meanwhile, it can be interpreted that transect_ID = 25 has *EPR* of 0.46 m/year during the period 1978 to 2017 and *LMS* rounded to 0.26 m/year. The linear regression equation for transect_ID = 25 (y = 0.5419x - 1050.9) was determined by plotting the shoreline positions with

respect to time (in years) and the slope of the equation describing the line; from this, the rate of *LRR* is 0.54 m/year and the *LCI90* is 0.80. The band of confidence around the reported rate of change is 0.54 ± 0.80. In other words, there is 90% confidence that the true rate of change is between -0.26 m/year and 1.34 m/year, with *LR2* of 0.46 and LSE of 7.57 m.

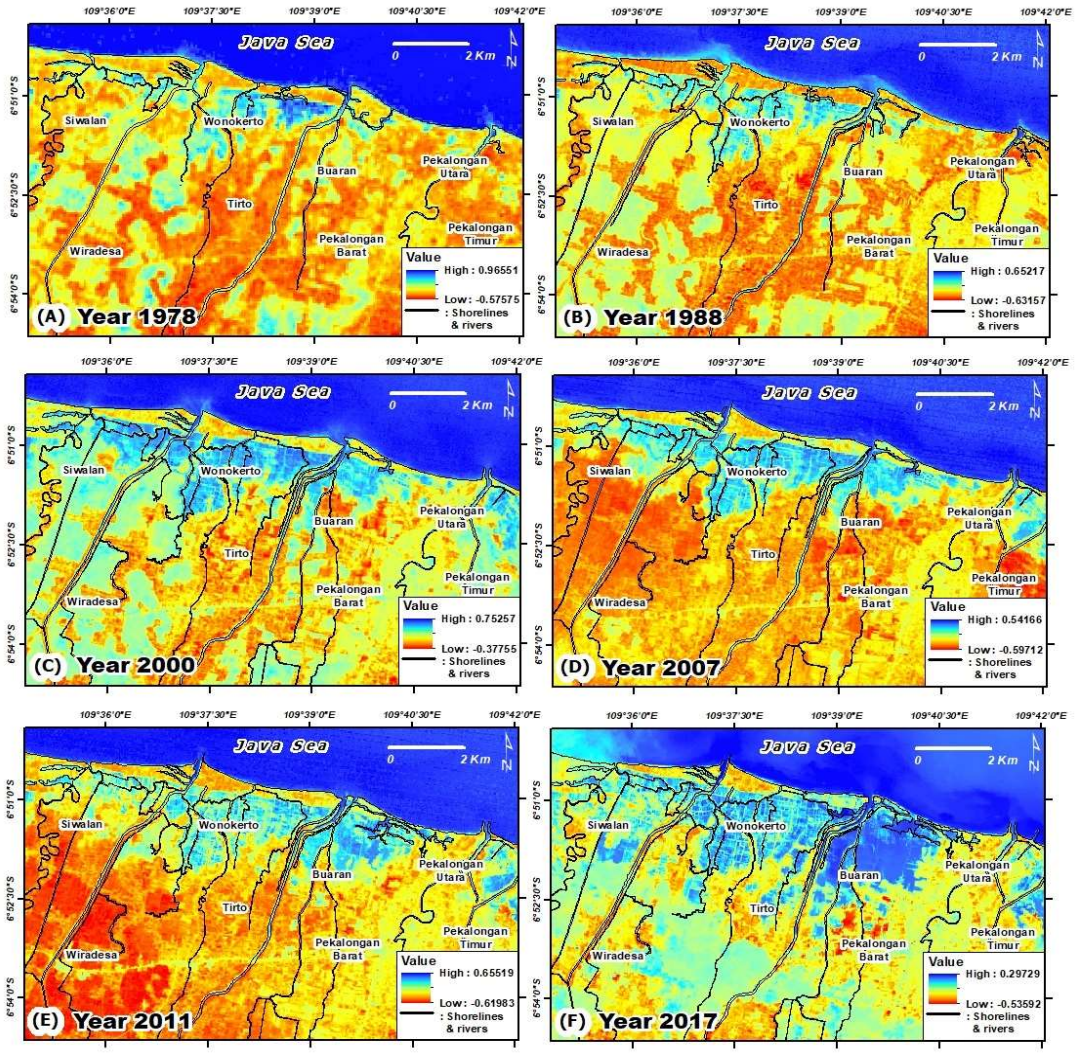

Figure 2 Normalized difference water index (NDWI) values for Landsat images were used as an indication of the separation of land and water bodies, and this data is used for shoreline and river extraction: (A) NDWI from Landsat MSS, 1978; (B) NDWI from Landsat 5 TM, 1988; (C) NDWI from Landsat 7 ETM+, 2000; (D) NDWI from Landsat 5 TM, 2007; (E) NDWI from Landsat 5 TM, 2011; (G) NDWI from Landsat 8 OLI/TIR, 2017

Table 1. NDWI values for the masking operation for land and water-body extraction from Landsat images for 1978 to 2017

Landsat images (years)	Statistics				Threshold masking Operation
	Min	Max	Mean	Std Dev	
1978	-0.58	0.97	0.05	0.44	0.34
1988	-0.63	0.65	-0.09	0.32	0.22
2000	-0.38	0.75	0.19	0.28	0.18
2007	-0.60	0.54	-0.15	0.30	0.20
2011	-0.62	0.60	-0.15	0.34	0.24
2017	-0.54	0.30	-0.10	0.18	0.08

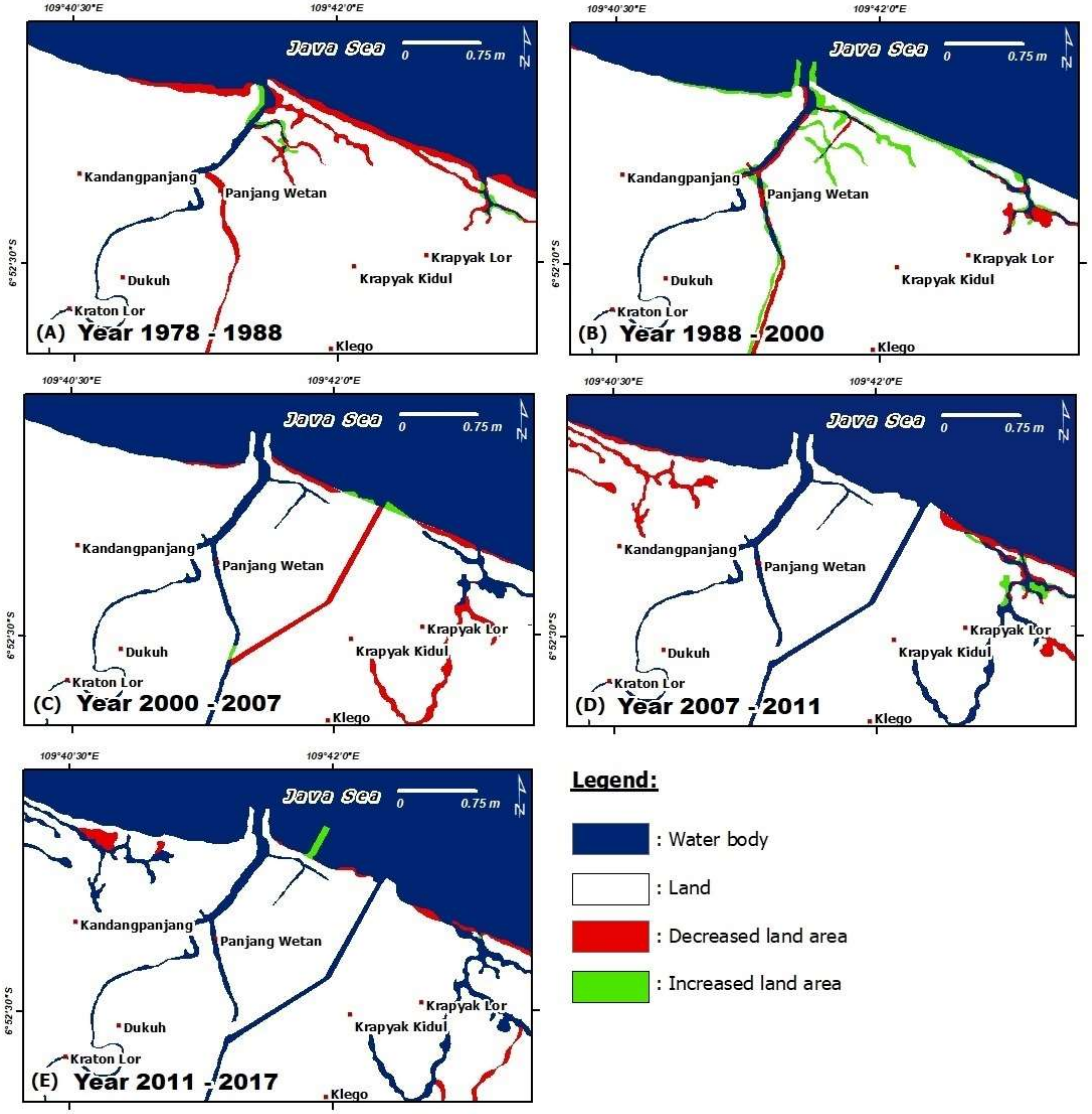

Figure 3. The results of land and water-body separation analysis in the eastern part of the study area and its multi-temporal change analysis for 1978 to 2017 for the inset location shown in Figure 4: (A) change analysis for 1978 to 1988; (B) change analysis for 1988 to 2000; (C) change analysis for 2000 to 2007; (D) change analysis for 2007 to 2011; (E) change analysis for 2011 to 2017

Table 2. The calculation of change area and average change based on the multi-temporal analysis of land and water-body separation for 1978 to 2017

Year of change	Change area (ha)		Average change (ha/yr)	
	Increased	Decreased	Increased	Decreased
1978–1988	28.51	164.85	2.85	16.49
1988–2000	38.63	170.76	3.22	14.23
2000–2007	10.07	63.80	1.44	9.11
2007–2011	17.23	68.87	4.31	17.22
2011–2017	11.67	75.66	1.95	12.61
Total	106.11	543.94	2.72	13.95

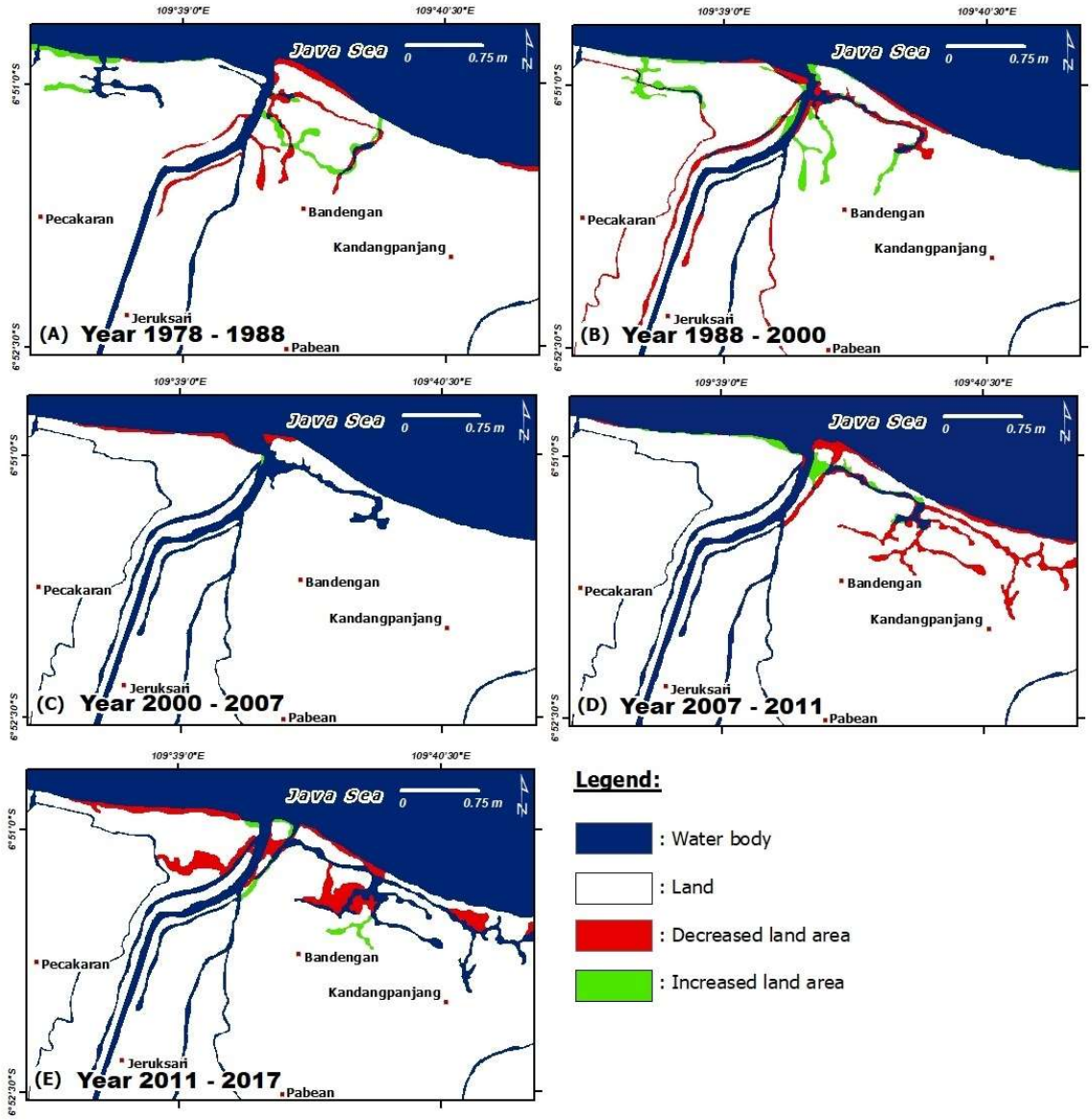

Figure 4. The results of land and water-body separation analysis for the central part of the study area and its multi-temporal change analysis for 1978 to 2017 for the inset location shown in Figure 4: (A) change analysis for 1978 to 1988; (B) change analysis for 1988 to 2000; (C) change analysis for 2000 to 2007; (D) change analysis for 2007 to 2011; (E) change analysis for 2011 to 2017

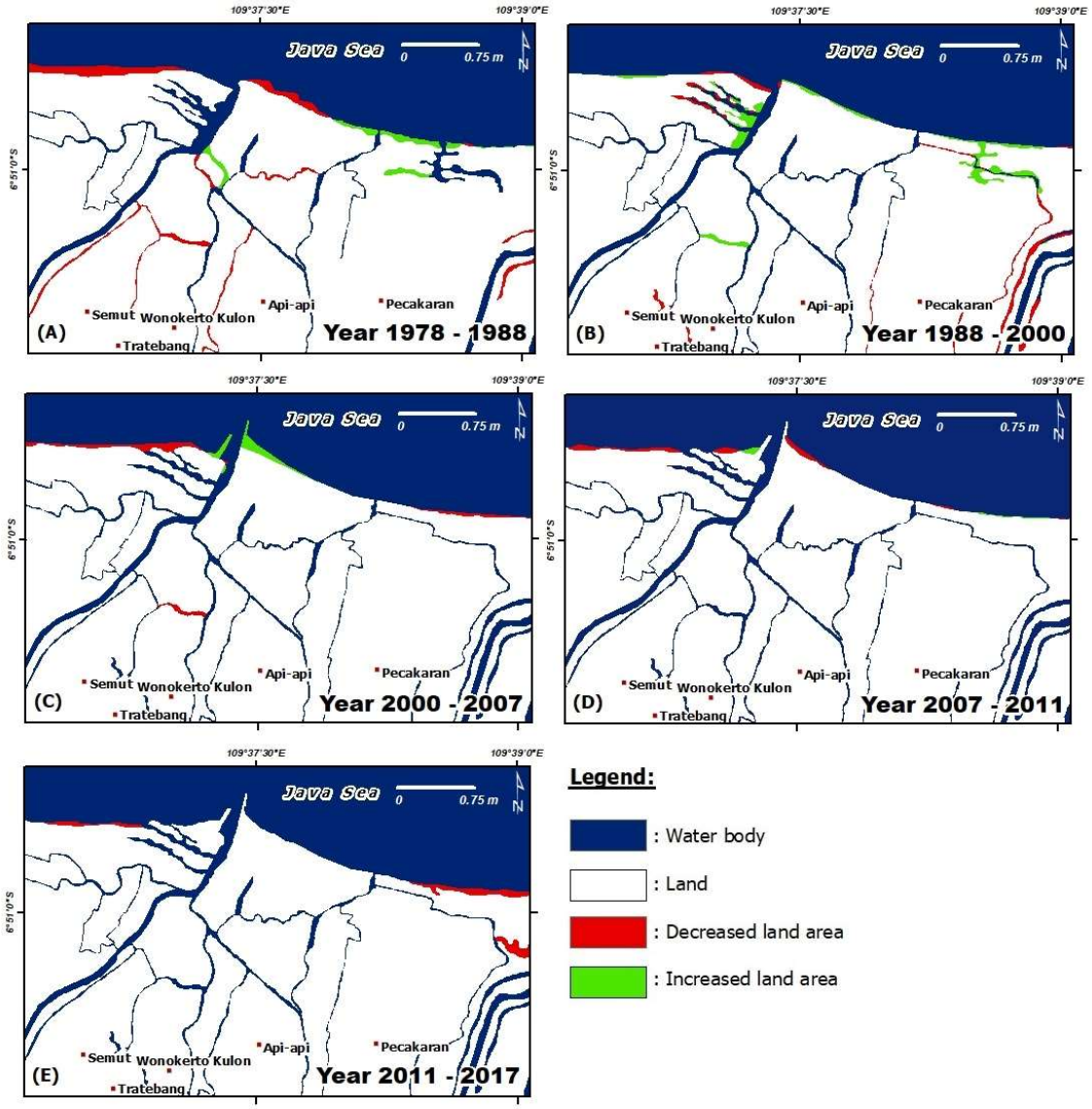

Figure 5. The results of land and water-body separation analysis for the western part of the study area and its multi-temporal change analysis for 1978 to 2017 for the inset location shown in Figure 4: (A) change analysis for 1978 to 1988; (B) change analysis for 1988 to 2000; (C) change analysis for 2000 to 2007; (D) change analysis for 2007 to 2011; (E) change analysis for 2011 to 2017

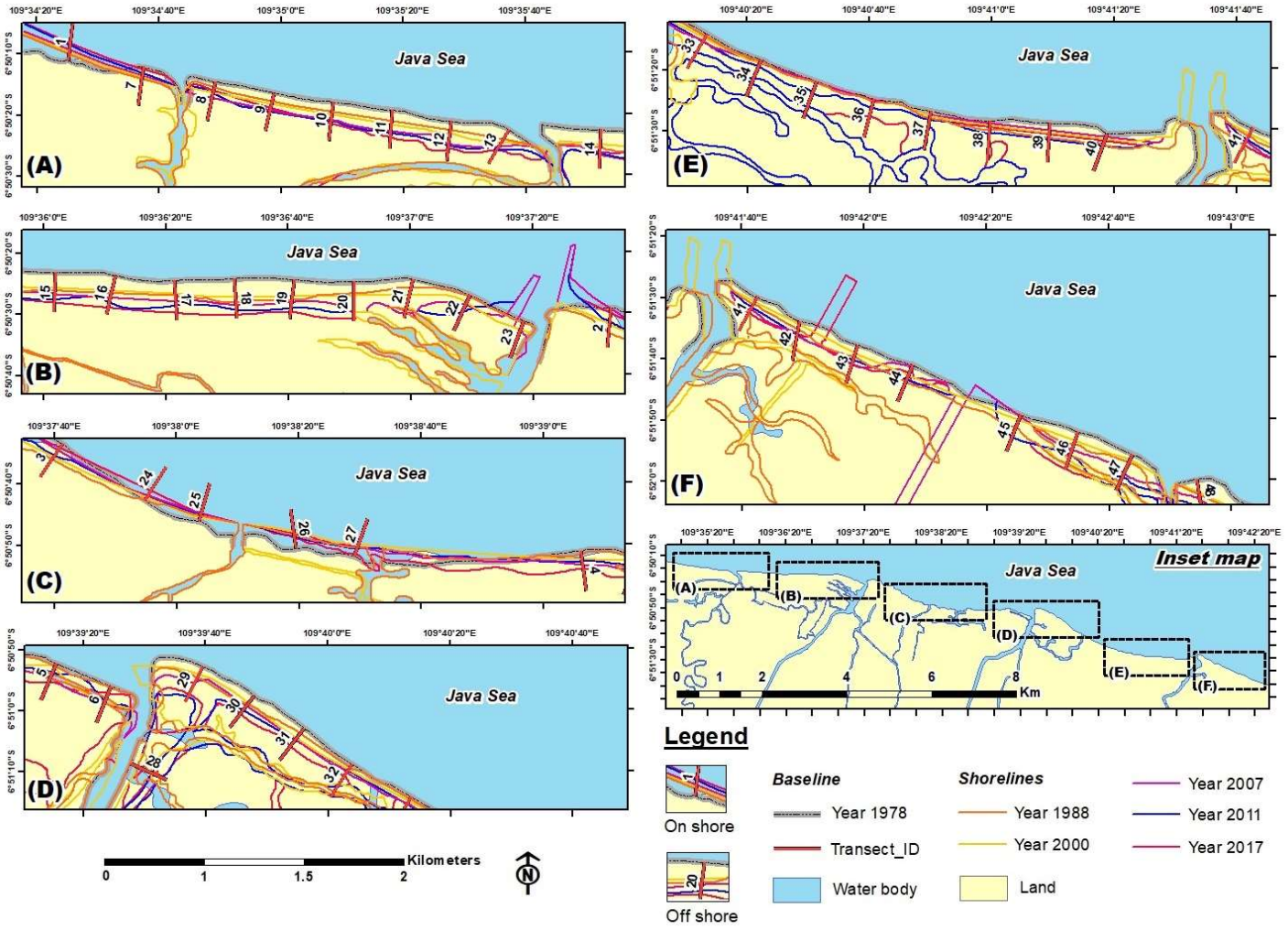

Figure 6. Segments and transects for DSAS in the study area

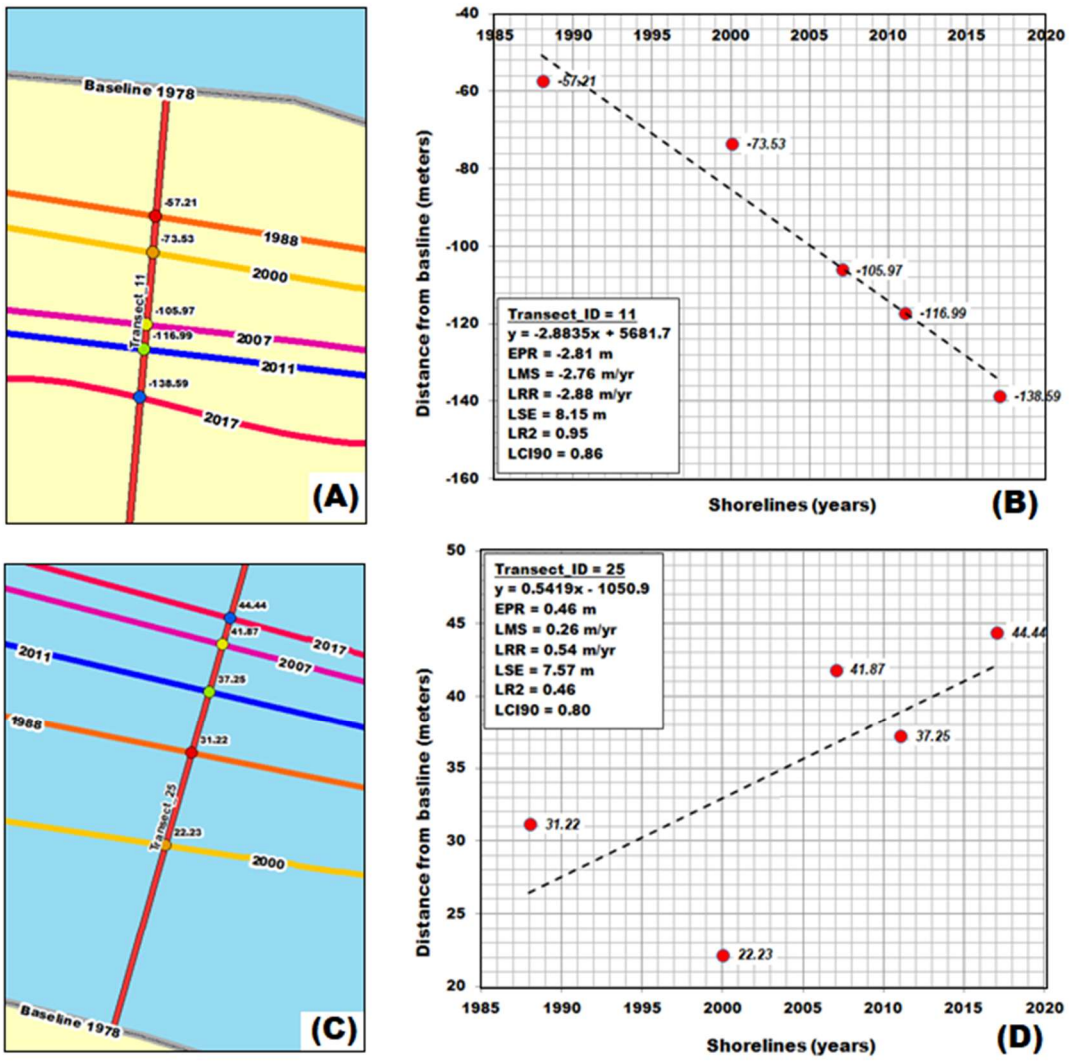

Figure 7. Examples: DSAS results for transect_ID = 11 (offshore position or erosion) and transect_ID = 25 (Onshore position or sedimentation) in the study area. (A) Shoreline position plotting for transect_ID = 11; (B) Linear regression equation for transect_ID = 11 (y = -2.8835x + 5661.7) was determined by plotting the shoreline positions with respect to time (years) and the slope of the equation describing the line is a rate of -2.88 m/year; (C) Shoreline position plotting for transect_ID = 25; (D) Linear regression equation for transect_ID = 25 (y = 0.5419x - 1050.9) with rate of 0.54 m/year

Table 3. Analysis of rate-change statistics provided by DSAS as used in this study

ID	**Change Statistics**					
	EPR	***LMS***	***LRR***	***LR2***	***LSE***	***LCI90***
1	1.89	3.10	1.95	0.89	8.76	0.92
2	-3.42	-3.28	-3.33	0.62	33.36	3.52
3	-2.50	-2.92	-2.23	0.71	18.37	1.94
4	-2.60	-2.91	-2.38	0.86	12.49	1.32
5	-0.71	-2.73	-0.61	0.04	37.00	3.91
6	-1.71	-0.10	-1.29	0.38	21.06	2.22
7	-1.67	-1.28	-1.59	0.86	8.24	0.87
8	-0.60	-0.60	-0.83	0.24	19.07	2.01
9	-1.15	-2.24	-1.60	0.69	13.91	1.47
10	-2.01	-2.04	-2.13	0.95	6.12	0.65
11	-2.81	-2.76	-2.88	0.95	8.15	0.86
12	-3.36	-3.46	-3.63	0.93	13.02	1.37
13	-2.27	-2.34	-2.45	0.96	6.05	0.64
14	-1.24	-1.28	-1.55	0.63	15.16	1.60
15	-2.10	-4.41	-2.31	0.68	20.29	2.14
16	-2.66	-5.20	-2.80	0.74	21.60	2.28
17	-3.00	-5.73	-3.03	0.74	22.87	2.41
18	-2.11	-5.61	-2.35	0.56	26.98	2.85
19	-2.10	-5.10	-2.30	0.60	23.97	2.53
20	-4.35	-0.94	-4.07	0.78	28.03	2.96
21	-0.28	-0.28	-1.20	0.09	48.27	5.09
22	-2.85	-2.89	-3.05	0.93	10.39	1.10
23	-4.46	-0.23	-4.28	0.67	38.62	4.08
24	2.03	1.07	1.74	0.83	9.99	1.05
25	0.46	0.26	0.54	0.46	7.57	0.80
26	0.43	2.04	0.48	0.20	12.37	1.31
27	1.23	3.25	1.10	0.37	18.64	1.97
28	-0.94	-0.09	-0.66	0.33	12.22	1.29
29	-3.24	-7.02	-4.05	0.63	39.99	4.22
30	-2.11	-4.33	-2.16	0.70	18.32	1.93
31	-2.79	-1.87	-2.51	0.91	10.25	1.08
32	-0.17	-0.62	-0.20	0.39	3.15	0.33
33	-4.82	-6.24	-5.31	0.72	43.04	4.54
34	-6.42	-8.14	-7.00	0.62	70.43	7.43
35	-5.59	-7.05	-6.13	0.59	65.45	6.91
36	-2.64	-2.62	-2.27	0.51	28.58	3.02
37	-4.72	-5.74	-5.24	0.52	65.51	6.91
38	-0.56	-0.56	-0.13	0.01	22.83	2.41
39	-0.63	-0.63	-0.29	0.03	21.57	2.28
40	-0.53	-0.53	-0.15	0.01	23.81	2.51
41	-0.07	-2.91	-0.03	0.00	30.76	3.25
42	-0.79	0.00	-0.77	0.69	6.59	0.70
43	-2.30	-1.15	-1.43	0.16	42.98	4.54
44	-1.39	-0.47	-1.19	0.21	29.43	3.11
45	-1.87	-2.35	-2.11	0.22	51.70	5.46
46	-0.91	-0.90	-0.02	0.00	31.63	3.34
47	-0.34	-0.18	-0.32	0.52	3.99	0.42
48	-3.57	-7.22	-3.77	0.72	30.60	3.23
49	-2.73	-5.61	-2.69	0.65	25.47	2.69

ID = transect ID; *EPR* = end point rate; *LMS* = least median of squares rate; *LRR* =linear regression rate; *LR2* = R-squared of linear regression; *LSE* = standard error of linear regression; *LCI90* = confidence interval of linear regression (for 90%)

Discussion

The coastal environment is an area that is related to land and sea. The change dynamics are caused by several physical processes such as tidal inundation, sea level rise, land subsidence, and erosion-sedimentation. These processes have an important role to play in the development of landscape and shoreline changes (Marfai et al., 2007). Urban development in coastal areas, such as the building of sea walls, breakwater, land reclamation, and removal of beach material from the coastline can also cause problems of environmental degradation and increased the vulnerability of coastal areas (Ongkosongo 1980; Mills et al., 2005; Marfai et al., 2007). The phenomenon of shoreline change is one of the most frequent problems encountered in the coastal environment and is caused by natural processes that result in dynamic changes in the coastal area. Coastal area change can affect the vulnerability of the coastal environment and its properties, such as shoreline stabilization, flood control, sediment retention, natural protection and others.

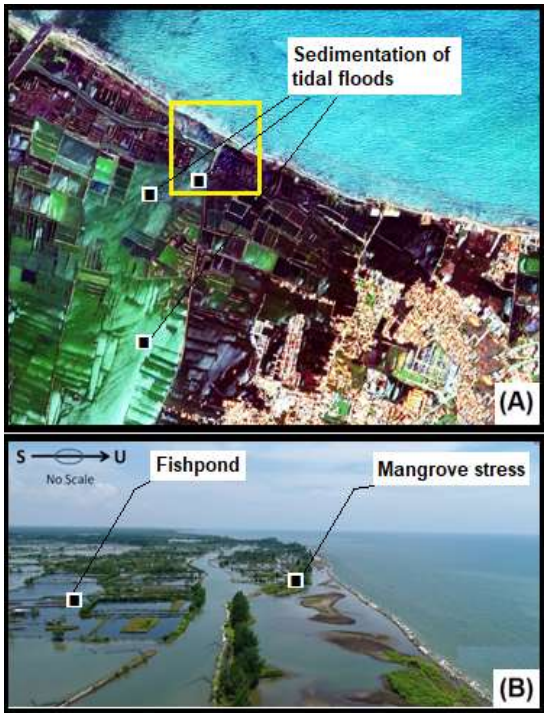

Figure 8. Effect of shoreline changes that contribute to tidal flooding in the study area. (A) Sedimentation as a trace of the impact of tidal flooding (Source: mosaic of SPOT6/7 satellite imagery in 2017 from LAPAN). (B) Indicate erosion of shoreline changes in several conditions such as stress mangroves and fishpond areas that are damaged due to the effects of tidal flooding, field conditions in 2017 (Photo: Yulianto, 2017).

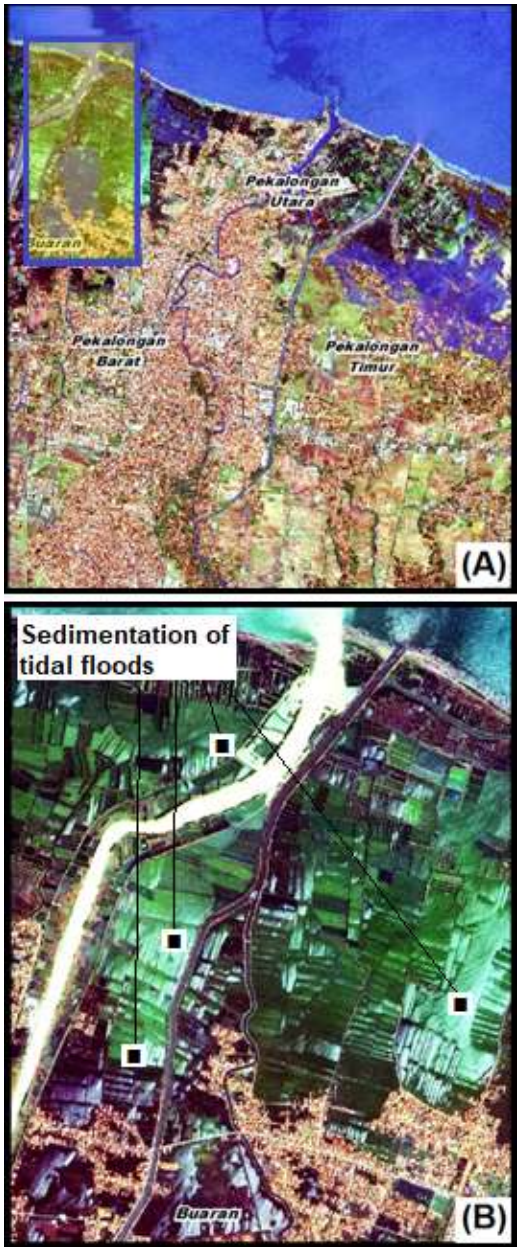

Figure 9. Impact of the influence of the construction of river lines that contribute to changes in coastline and cause tidal flooding in the study area. (A) and (B) Sedimentation as a trace of the impact of tidal flooding (Source: mosaic of SPOT6/7 satellite imagery in 2017 from LAPAN).

In this study, the method of integrating remote sensing data and GIS has been widely used to monitor and analyze the dynamics of shoreline change. Using various methods, some researchers such as Ozdarici and Turker (2006), Chalabi et al. (2006), Xiaodong et al. (2006) and others. The analysis of shoreline changes was performed using the DSAS and it can be seen that the pattern of coastline change tends to be dominated by offshore erosion. The impact of coastline changes that occur

naturally and also because of the development activities from 1978 to 2017 have contributed to the causes of tidal flooding in the study area. This is also shown in Figure 8 and Figure 9, related to conditions in the field and changes that occur at this time. Some efforts can be made to prevent the worsening of coastline changes that have an impact on tidal flooding, namely:(a) recovery of the natural conditions of the coastal region with the reconstruction and revitalization of natural "barriers" or the mangrove planting, which serve to inhibit, reduce or absorb water due to flood tides, (b) The release of coastal land or estuary as a conservation area, and rearrangement of ponds around the river/coastal estuary, (c) strengthen the wave retaining sandbags embankments that have existed along the coast.

Conclusion

In this study, remote sensing data integrated with GIS techniques have been successfully used to track and map historically the dynamics of shoreline change. An approach combining spectral value NDWI and visual interpretation of Landsat images was used and proposed to indicate the separation of land and water bodies, for shoreline extraction. The analysis of shoreline changes was performed using the DSAS and it can be seen that the pattern of coastline change tends to be dominated by offshore erosion. The results of this study may also be important as input data for coastal hazard assessment as part of the effort to overcome the problem of flood tides and also as a consideration in studying the vulnerability of the coastal environment. In addition, the results of this study are supported by spatial data information at a mapping scale of 1:25,000. For the next research could be carried out using information from other remote sensing data (SPOT 6/7, Pleiades, Ikonos, Quick bird and others) to support spatial data information at mapping scales of 1:5,000 to 1:10,000.

Acknowledgements

This paper is part of the research activities entitled 'The utilization of remotely sensed data to support analysis of flooding in Indonesia'. This research was funded by the budget of DIPA LAPAN activities in 2018, Remote Sensing Application Center, Indonesian National Institute of Aeronautics and Space (LAPAN). Thanks go to Dr Mujio Sukir, Dr. Indah Prasasti, Gigih Giarrastowo and Tival Gorodas and colleagues at the Remote Sensing Application Center, LAPAN, for their support, discussions and suggestions. Landsat 5 MSS and Landsat 7 TM images were provided by the US Geological Survey (USGS), Landsat 8 OLI/TIR images were provided by Remote Sensing Technology and Data Center, LAPAN and topographic maps were provided by the Indonesian Geospatial Information Agency (BIG).

References

Addo, K.A., Jayson, Q.P.N. and Kufogbe, K.S. 2011. Quantitative analysis of shoreline change using medium resolution satellite imagery in Keta, Ghana. *Marine Science* 1(1):1-9. DOI: 10.5923/j.ms.20110101.01.

Allen, T.R. 2012. Estimating coastal lagoon tidal flooding and repletion with multidate ASTER thermal imagery. *Remote Sensing*, 4:3110-3126. DOI:10.3390/rs4103110.

Bird, E.C.F. and Ongkosongo, O.S.R. 1980. Environmental changes on the coasts of Indonesia. The United Nations University: United Nations University Press.

Bonetti, J., Henrique, A., da Fountoura, K., Mariela, M., Clarissa, B., Guilherme, V., Tolda, Jr. E.E. and Mauricio, G. 2013. Spatial and numerical methodologies on coastal erosion and flooding risk. *Coastal Hazards, Research Library* 6:423-442.

Brown, N., Nicholls, R.J., Collin, D.W., Hanson, S., Hinkel, J., Kebede, A.S., Neumann, B. and Vafieds, T.A. 2013. Seal level rise impacts and responses: a global perspective. *Coastal Hazards, Research Library* 6:117-149.

Burningham, H. and French, J. 2017. Understanding coastal change using shoreline trend analysis supported by cluster-based segmentation. *Geomorphology* 282:131-149.

Carrasco, A.R., Ferreira, Ó., Matias, A. and Freire, P. 2012. Natural and human-induced coastal dynamics at a back-barrier beach. *Geomorphology* 159/160:30-36, doi: 10.1016/ j.geomorph. 2012.03.001.

Chalabi, A., Mohd-Lokman, H., Mohd-Suffian, I., Karamali, K., Karthigeyan, V. and Masita, M. 2006. Monitoring shoreline change using Ikonos image and aerial photographs: a case study of Kuala Terengganu area, Malaysia. (ISPRS Mid-term Symposium Proceeding. May 2006, Enschede).

Chavez, P.S. Jr. 1988. An improved dark-object subtraction technique for atmospheric scattering correction of multispectral data. *Remote Sensing Environmental* 24:459–479.

Condon, W.H., Pardyanto, L., Ketner, K.B., Amin, T.C., Gafoer, S. and Samodra, H. 1996. Geological map scale 1:100.000 sheet Banjarnegara-Pekalongan. Second edition. Center for Geological Research and Development.

Ekercin, S. 2007. Coastline change assessment at the Aegean Sea coasts in Turkey using multitemporal landsat imagery. *Journal of Coastal Research* 23(3):691 – 698.

Erener, A. and Yakar, M. 2012. Monitoring coastline change using remote sensing and GIS technologies. International Conference on Earth Science and Remote Sensing Lecture Notes in Information Technology.

Erkkilä, A. and Kalliola, R. 2004. Patterns and dynamics of coastal waters in multi-temporal satellite images: support to water quality monitoring in the

Archipelago Sea, Finland. Estuarine. *Coastal and Shelf Science* 60(2):165-177.

Gao, B.C. 1996. NDWI - A Normalized difference water index for remote sensing of vegetation liquid water from space. *Remote Sensing Environmental* 58:257-266.

Hackney, C., Darby, S.E. and Leyland, J. 2013. Modelling the response of soft cliffs to climate change: A statistical, process-response model using accumulated excess energy. *Geomorphology* 187:108-121. doi: 10.1016/j.geomorph. 2013.01.005.

Kaichang, D., Ruijing, M., Jue, W. and Ron, L. 2004. Coastal mapping and change diction using high-resolution IKONOS satellite imagery. http://shoreline.eng.ohio-state.edu/ research/diggov/DigiGov.html.

Kuleli, T., Guneroglu, A., Karsli, F. and Dihkan, M. 2011. Automatic detection of shoreline change on coastal Ramsar wetlands of Turkey. *Ocean Engineering* 38(10):1141-1149.

Li, X. and Damen, M.C.J. 2010. Coastline change detection with satellite remote sensing for environmental management of the Pearl River Estuary, China. *Journal of Marine Systems* 82: S54–S61.

Marfai, M.A. and King, L. 2007. Monitoring land subsidence in Semarang, Indonesia. *Environmental Geology* 53:651-659, doi:10.1007/s00254-007-0680-3.

Marfai, M.A., Almohammad, H., Dey, S., Susanto, B. and King, L. 2007. Coastal dynamic and shoreline mapping: multi-sources spatial data analysis in Semarang Indonesia. *Environmental Monitoring and Assessment* 142(1-3):297-308, doi:10.1007/s10661-007-9929-2.

McFeeters, S.K. 1996. The use of the Normalized Difference Water Index (NDWI) in the delineation of open water features. *International Journal of Remote Sensing* 17:1425–1432.

McFeeters, S.K. 2013. Using the Normalized Difference Water Index (NDWI) within a Geographic Information System to detect swimming pools for mosquito abatement: a practical approach. *Remote Sensing* 5:3544–3561.

Memon, A.A., Muhammad, S., Rahman, S. and Haq, M. 2015. Flood monitoring and damage assessment using water indices: A case study of Pakistan flood - 2012. *The Egyptian Journal of Remote Sensing and Space Sciences* 18:99–106.

Mills, J.P., Buckley, S.J., Mitchell, H.L., Clarke, P.J. and Edwards, S.J. 2005. A geomatics data integration technique for coastal change monitoring. *Earth Surface Processes and Landforms* 30:651–664.

NASA 2011. Landsat 7 science data users handbook. Maryland: Landsat Project Science Office at NASA's Goddard Space Flight Center in Greenbelt.

Oyedotun, T.D.T. 2014. Shoreline geometry: DSAS as a tool for historical trend analysis. *Geomorphological Techniques*, Chap. 3, Sec. 2.2. ISSN 2047-0371

Ozdarici, A. and Turker, M. 2006. Comparison of different spatial resolution images for parcel-based crop mapping. (ISPRS Mid-term Symposium Proceeding. May 2006, Enschede).

Rio, L.D., Gracia, J.F. and Benavente, J. 2013. Shoreline change patterns in sandy coasts. A case study in SW Spain. *Geomorphology* 196:252-266, doi:10.1016/j.geomorph.2012.07.027.

Shalaby, A. and Tateishi, R. 2007. Remote sensing and GIS for mapping and monitoring land cover and land-use changes in the Northwestern coastal zone of Egypt. *Applied Geography*2 7(1):28-41.

Thébaudeau, B., Trenhaile, A.S. and Edwards, R.J. 2013. Modelling the development of rocky shoreline profiles along the northern coast of Ireland. *Geomorphology* 203:66-78, doi: 10.1016/j.geomorph.2013.03.027.

Thieler, E.R., Himmelstoss, E.A., Zichichi, J.L. and Ayhan, E. 2017. Digital Shoreline Analysis System (DSAS) version 4.0 - An ArcGIS extension for calculating shoreline change (ver.4.4, July 2017): U.S. Geological Survey Open-File Report 2008-1278.

Thomas, T., Rangel-Buitrago, N., Phillips, M.R., Anfuso, G. and Williams, A.T. 2015. Mesoscale morphological change, beach rotation and storm climate influences along a macrotidal embayed beach. *Journal of Marine Science and Engineering* 3:1006-1026.

USGS 2013a. Landsat missions: frequently asked questions about the Landsat missions US Geological Survey. Last modified: 5/30/123. Landsat.usgs.gov.

USGS 2013b. Using the US Geological Survey Landsat 8 product. Last modified: 5/30/123. Landsat7.usgs.gov.

Xiaodong, Z., Ya, G.J. and Deren, L. 2006. A strategy of change detection based on remotely sensed imagery and GIS data. ISPRS Mid-term Symposium Proceeding, Enschede.

Yulianto, F., Prasasti, I., Pasaribu, J.M., Fitriana, H.L., Zylshal, Haryani, N.S. and Sofan, P. 2016. The dynamics of land use/land cover change modeling and their implication for the flood damage assessment in the Tondano watershed, North Sulawesi, Indonesia. *Modeling Earth System Environmental* 2:47, doi:10.1007/s40808-016-0100-3.

Zhao, B., Guo, H., Yan, Y., Wang, Q. and Li, B. 2008. A simple waterline approach for tidelands using multi-temporal satellite images: A case study in the Yangtze Delta. Estuarine, *Coastal and Shelf Science* 77(1):134-142.